

# Buckling analysis of sandwich beam rested on elastic foundation and subjected to varying axial in-plane loads

Mostafa A. Hamed<sup>\*1</sup>, Salwa A Mohamed<sup>2a</sup> and Mohamed A. Eltahaer<sup>1,3b</sup>

<sup>1</sup>Mechanical Engineering Department, Faculty of Engineering, King Abdulaziz University, P.O. Box 80204, Jeddah, Saudi Arabia

<sup>2</sup>Department of Engineering Mathematics, Faculty of Engineering, Zagazig University, P.O. Box 44519, Zagazig, Egypt

<sup>3</sup>Mechanical Design & Production Department, Faculty of Engineering, Zagazig University, P.O. Box 44519, Zagazig, Egypt

(Received August 17, 2019, Revised November 26, 2019, Accepted December 12, 2019)

**Abstract.** The current paper illustrates the effect of in-plane varying compressive force on critical buckling loads and buckling modes of sandwich composite laminated beam rested on elastic foundation. To generalize a proposed model, unified higher order shear deformation beam theories are exploited through analysis; those satisfy the parabolic variation of shear across the thickness. Therefore, there is no need for shear correction factor. Winkler and Pasternak elastic foundations are presented to consider the effect of any elastic medium surrounding beam structure. The Hamilton's principle is proposed to derive the equilibrium equations of unified sandwich composite laminated beams. Differential quadrature numerical method (DQNM) is used to discretize the differential equilibrium equations in spatial direction. After that, eigenvalue problem is solved to obtain the buckling loads and associated mode shapes. The proposed model is validated with previous published works and good matching is observed. The numerical results are carried out to show effects of axial load functions, lamination thicknesses, orthotropy and elastic foundation constants on the buckling loads and mode shapes of sandwich composite beam. This model is important in designing of aircrafts and ships when non-uniform compressive load and shear loading is dominated.

**Keywords:** buckling stability; in-plane load function; sandwich beams; unified beam theories; elastic foundations; Differential Quadrature Method (DQM)

## 1. Introduction

Recently, composite orthotropic laminated beam (COLB) and plate (COLP) structures have been used in enormous engineering applications, such as, in military, civil, mechanical, and aeronautical industries. Composite laminated structure has applicability to tolerate its strength, rigidity, stiffness and weight specifications. Thus, many researchers and engineers focused their researches and adopted different theories to illustrate bending, shearing, buckling, free and forced vibration behaviors of composite beam structure.

In 2010, Kim *et al.* investigated the stability of thin-walled composite beam subjected to eccentric constant axial force, end moments, and linearly varying axial force. Sedighi *et al.* (2012a, b) used analytical method to obtain the exact solution of dynamic behavior of the nonlinear vibration of buckled beam. Assie *et al.* (2011) developed numerical model to analyze the dynamical response of orthotropic viscoelastic COLP in time domain by using the

integral form of generalized Wiechert model. Eltahaer *et al.* (2012, 2013a, b) investigated mechanical responses of functionally graded (FG) nanobeam structure by using differential constitutive form of Eringen model. Simsek and Reddy (2013) exploited higher order beam theories and modified couple stress to illustrate the buckling of FG microbeam embedded in Pasternak elastic medium. Eltahaer *et al.* (2014a, b) modified previous model by considering shear effect to illustrate the mechanical bending, buckling and vibrational behaviors of thick nanobeams. Khater *et al.* (2014) investigated the impact of surface energy and thermal loading on the static stability of nanowires. Emam and Eltahaer (2016) investigated buckling and post-buckling of composite beams in hydrothermal environments due to temperature variation and moisture absorption assuming temperature-moisture-dependent. She *et al.* (2017, 2018a) exploited refined beam model to study a thermal buckling and post-buckling of FG tubes subjected to a temperature and resting on elastic foundations. She *et al.* (2018b) predicted wave propagation of FG porous Reddy nanobeams in conjunction with the non-local strain gradient theory.

Mohamed *et al.* (2018) developed differential quadrature procedure to forecast nonlinear forced vibration of curved beam in locality of post-buckling modes. Dehrouyeh-Semnani (2018) presented an analytical to investigate the non-linear response of curved FG beams subjected to induced temperature. Emam *et al.* (2018) investigated the post-buckling and free vibration behaviors

\*Corresponding author, Professor  
E-mail: mhamed@kau.edu.sa

<sup>a</sup> Ph.D.  
E-mail: sa\_mohamed@zu.edu.eg

<sup>b</sup> Ph.D. Student  
E-mail: meltahaer@kau.edu.sa

of imperfect composite nanobeams by using nonlocal elasticity differential model of Eringen. Bessaim *et al.* (2018) exploited a refined hyperbolic shear deformation theory to study buckling behaviors of nano-size FG beams embedded in elastic media. Eltaher *et al.* (2019a) predicted nonlinear post-buckling behaviors of curved carbon nanotube embedded in nonlinear elastic foundation by using modified energy equivalent model. Eltaher *et al.* (2019b) derived nonlinear integro-partial-differential equation of periodic and aperiodic configuration buckled beam to study nonlinear vibration behaviors of buckled imperfect beam. She *et al.* (2019a, b) employed nonlocal strain gradient theory to investigate snap-buckling of FG curved nanobeams under uniform temperature distributions across the thickness. Li *et al.* (2019) investigated thermal post-buckling of sandwich honeycomb cores beams with FG negative Poisson's ratio. Hamed *et al.* (2019) studied the effect of porosity on static and dynamic of FG nanobeams. Abdalrahmaan *et al.* (2019) and Almitani *et al.* (2019) studied free and forced vibration of perforated beams with Euler and Timoshenko beam theories. Akbas (2019a, b) investigated the post-buckling of laminated composite and FG beams under hygrothermal effects by using finite element method. Mohamed *et al.* (2019) studied the effect of imperfection on static buckling of carbon nanotube rested on nonlinear elastic foundation.

In real applications, such as, the aircraft wing, the stiffened plate in the ship structure, slabs of a multi-story building, the applied axial compressive loads are nonuniform distributed through the axial direction. Thus, the stability and mechanical behaviors of composite beam structure under the action of varying axial load are the main interest of many researchers. Farajpour *et al.* (2012) presented buckling response of orthotropic single layered graphene sheet under linearly varying in-plane load by using nonlocal continuum mechanics. Mijušković *et al.* (2014) derived exact stress functions to study static stability of isotropic plates under uniaxial and biaxial compression. Sedighi and Daneshmand (2014) presented the high order frequency-amplitude relationship for nonlinear transversely vibrating beams with odd and even nonlinearities, using Homotopy perturbation method. Jun *et al.* (2016, 2017) exploited dynamic stiffness method and shear deformation theory to analyze the buckling and free vibration of axially loaded COLB. Akbas (2018a, b) investigated static and postbuckling behaviors of geometrically nonlinear simply supported laminated composite beam subjected to a non-follower transversal point load at the midpoint of the beam. Akbas (2018c) investigated nonlinear static response of laminated composite beams under nonuniform temperature effects with temperature dependent physical properties. Karamanli and Aydogdu (2019) studied elastic buckling of isotropic, laminated composite and sandwich beams under numerous axially varying in-plane forces based on a modified shear deformable beam theory. Shimpi *et al.* (2019) presented two variables refined shear beam theory to study static bending and free vibrations of isotropic rectangular beams. Eltaher *et al.* (2020) investigated the buckling behavior of composite beam under varying in-plane load by using unified beam theories.

According to literature review and author's knowledge no researchers have attempted to investigate the static stability of sandwich orthotropic laminated unified beam rested on elastic foundation under varying in-plane loads. This study aims to fulfill this gap. Different distributions of in-plane load are included in the study. The Winkler and Pasternak elastic foundations are introduced. The differential quadrature method (DQM) is exploited as numerical method to solve the governing equilibrium equations.

The paper is organized as follows: Section 2 presents the problem formulation, that includes axial load distribution functions, kinematics displacement assumptions of unified beam theories, constitutive equations of sandwich beams, and derived equilibrium equations. Section 3 presents the solution procedure and discretization method of the beam structure using differential quadrature method. Section 4 is devoted to validation and parametric studies to preset effects of beam theories, type of loading, sandwich geometry, slenderness ratio, and elastic foundations on critical buckling loads. Main remarks and conclusion points are summarized and presented through section 5.

## 2. Problem formulation

The geometrical presentation of clamped-clamped sandwich composite beam rested on elastic foundation and subjected to axial distributed in-plane axial load are presented in Fig. 1.

### 2.1 In-plane load function

The variation of in-plane load in longitudinal direction has many practical applications such as the stiffened panel of aircraft wing. So, the axial force can be assumed to be constant, linear, and parabolic in the longitudinal direction. The proposed function depicting the variation of in-plane load through the longitudinal direction, can be represented as [Karamanli and Aydogdu (2019)]

$$N_{axial}(x) = N_{amp} \left[ \alpha_0 + \alpha_1 \left( x + \frac{l}{2} \right) + \alpha_2 \left( x + \frac{l}{2} \right)^2 \right] = N_{amp} C(x) \quad (1)$$

where  $N_{amp}$  is the load amplitude. It is assumed that the positive load is a compressive. The distribution of external loads can be controlled by constant coefficients ( $\alpha_i$ ) of the polynomial described in Eq. (1). To conform results of any profile of load distribution, the integral of the each axially variable in-plane load through the length of the beam is equal to integral of the uniformly distributed in-plane load, Karamanli and Aydogdu (2019). Table 1 shows the value of load profile coefficients described in Eq. (1).

### 2.2 Displacement field of unified beam

Based on unified shear deformation that was proposed in 1993 by Soldatos and Timarci, displacement field of sandwich beam can be described by [Simsek and Reddy (2013) and Jun *et al.* (2016)]

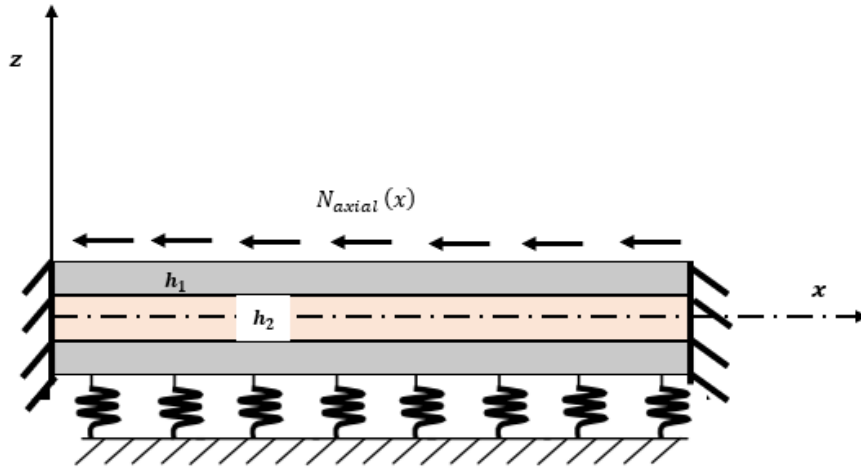


Fig. 1 Sandwich composite beam rested on elastic foundation and subjected to a distributed in-plane axial load

Table 1 Coefficients of the axial varying load functions

Load function	Load Symbol	$\alpha_0$	$\alpha_1$	$\alpha_2$
Constant Load	$N_{con}$	1	0	0
Linear Load-zero from left side	$N_{LL}$	0	2	0
Linear Load-zero from right side	$N_{LR}$	2	-2	0
Parabolic Load-zero from left side	$N_{PL}$	0	0	3
Parabolic Load-zero from right side	$N_{PR}$	3	-6	3
Symmetric Parabolic Load	$N_{PS}$	0	6	-6

$$u(x, z) = u_0(x) - z \frac{\partial w_0(x)}{\partial x} + f(z)\varphi(x) \quad (2a)$$

$$w(x, z) = w_0(x) \quad (2b)$$

in which the axial in-plane and transverse out of plane displacements are where  $u$  and  $w$ . However,  $u_0$  and  $w_0$  are axial and transverse displacements along the mid-plane of the beam, respectively.  $\varphi$  is the rotation of the normal to the mid-plane.  $f(z)$  is a function describing the shear deformation along the  $z$ -axis and satisfying the zero shear at the top and bottom surfaces. Based on beam shear theories, the shear functions are depicted by

$$\text{Parabolic shear deformation beam theory (PSDBT)} \quad (3a)$$

$$f(z) = z \left( 1 - \frac{4z^2}{3h^2} \right)$$

$$\text{Exponential shear deformation beam theory (ESDBT)} \quad (3b)$$

$$f(z) = ze^{-2(z/h)^2}$$

$$\text{Trigonometric shear deformation beam theory (TSDBT)} \quad (3c)$$

$$f(z) = \left( \frac{h}{\pi} \right) \sin(\pi z/h)$$

$$\text{Hyperbolic shear deformation beam theory (HSDBT)} \quad (3d)$$

$$f(z) = h \sinh(z/h) - z \cosh(1/2)$$

Strains accompanying with displacement fields, which defined by Eqs. (2) and (3) can be represented by

$$\varepsilon_x = \varepsilon_x^0 + zk_x^0 + f(z)k_x^2 \quad (4a)$$

$$\gamma_{xz} = g(z)k_{xz}^s \quad (4b)$$

in which  $\varepsilon_x$  and  $\gamma_{xz}$  are the normal and shear strains respectively. The other normal ( $\varepsilon_y, \varepsilon_z$ ) and shear ( $\gamma_{xy}, \gamma_{yz}$ ) strain components are zeros. The element components of normal and shear strain described in Eq. (4) can be written as

$$\varepsilon_x^0 = \frac{\partial u_0}{\partial x}, \quad k_x^0 = -\frac{\partial^2 w_0}{\partial x^2}, \quad k_x^2 = \frac{\partial \varphi}{\partial x}, \quad (5)$$

$$k_{xz}^s = \varphi \quad \text{and} \quad g(z) = \frac{\partial f}{\partial z}$$

### 2.3 Constitutive of laminated structure

The stress-strain equations orient along lamina coordinates can be represented for in plane stress components and intra-laminar shear stress components as following, Assie *et al.* (2011)

$$\begin{Bmatrix} \sigma_x \\ \sigma_y \\ \sigma_{xy} \end{Bmatrix} = \begin{bmatrix} \bar{Q}_{11} & \bar{Q}_{12} & \bar{Q}_{16} \\ \bar{Q}_{12} & \bar{Q}_{22} & \bar{Q}_{26} \\ \bar{Q}_{16} & \bar{Q}_{26} & \bar{Q}_{66} \end{bmatrix} \begin{Bmatrix} \varepsilon_x \\ \varepsilon_y \\ \gamma_{xy} \end{Bmatrix} \quad (6a)$$

$$\begin{Bmatrix} \sigma_{yz} \\ \sigma_{xz} \end{Bmatrix} = \begin{bmatrix} \bar{Q}_{44} & \bar{Q}_{45} \\ \bar{Q}_{45} & \bar{Q}_{55} \end{bmatrix} \begin{Bmatrix} \gamma_{yz} \\ \gamma_{xz} \end{Bmatrix} \quad (6b)$$

in which the transformed reduced stiffness material constants at any fiber orientation angle ( $\theta$ ) can be given by, Reddy (2003)

$$\begin{aligned} \bar{Q}_{11} = & Q_{11} \cos^4(\theta) + \\ & 2[Q_{12} + 2Q_{66}] \sin^2(\theta) \cos^2(\theta) + Q_{22} \sin^4(\theta) \end{aligned} \quad (7a)$$

$$\begin{aligned} \bar{Q}_{12} = & [Q_{11} + Q_{22} - 4Q_{66}] \sin^2(\theta) \cos^2(\theta) \\ & + Q_{12} [\sin^4(\theta) + \cos^4(\theta)] \end{aligned} \quad (7b)$$

$$\begin{aligned} \bar{Q}_{22} = & Q_{11} \sin^4(\theta) + 2[Q_{12} + 2Q_{66}] \sin^2(\theta) \cos^2(\theta) + \\ & Q_{22} \cos^4(\theta) \end{aligned} \quad (7c)$$

$$\begin{aligned} \bar{Q}_{16} = & [Q_{11} - Q_{12} - 2Q_{66}] \sin(\theta) \cos^3(\theta) \\ & + [Q_{12} - Q_{22} \\ & + 2Q_{66}] \sin^3(\theta) \cos(\theta) \end{aligned} \quad (7d)$$

$$\begin{aligned} \bar{Q}_{26} = & [Q_{11} - Q_{12} - 2Q_{66}] \sin^3(\theta) \cos(\theta) \\ & + [Q_{12} - Q_{22} \\ & + 2Q_{66}] \sin(\theta) \cos^3(\theta) \end{aligned} \quad (7e)$$

$$\begin{aligned} \bar{Q}_{66} = & [Q_{11} + Q_{22} - 2Q_{12} \\ & - 2Q_{66}] \sin^2(\theta) \cos^2(\theta) \\ & + Q_{66} [\cos^4(\theta) + \sin^4(\theta)] \end{aligned} \quad (7f)$$

and the transformed reduced shear stiffness material constants are represented by

$$\bar{Q}_{44} = Q_{44} \cos^2(\theta) + Q_{55} \sin^2(\theta) \quad (8a)$$

$$\bar{Q}_{55} = Q_{44} \sin^2(\theta) + Q_{55} \cos^2(\theta) \quad (8b)$$

$$\bar{Q}_{45} = [Q_{55} - Q_{44}] \sin(\theta) \cos(\theta) \quad (8c)$$

The material stiffness constant can be obtained in terms of engineering constants as

$$\begin{aligned} Q_{11} = & \frac{E_1}{1 - \nu_{12}\nu_{21}}, \quad Q_{12} = \frac{\nu_{12}E_2}{1 - \nu_{12}\nu_{21}}, \quad Q_{22} = \\ & \frac{E_2}{1 - \nu_{12}\nu_{21}}, \quad Q_{44} = G_{23}, \quad Q_{55} = G_{13}, \quad Q_{66} = G_{12} \end{aligned} \quad (9)$$

Based on the unified shear deformation beam theory, the force, the moment and unified bending moment resultants along the in-plane are defined by

$$\begin{Bmatrix} N \\ M \\ P \end{Bmatrix} = \begin{bmatrix} A & B & E \\ B & D & F \\ E & F & H \end{bmatrix} \begin{Bmatrix} \varepsilon^0 \\ k^0 \\ k^2 \end{Bmatrix} \quad (10)$$

However, the nonzero shear force can be described as function of shear strain and transformed shear rigidities by

$$R_{xz} = (F_{55} - F_{45}^2/F_{44})k_{xz}^s = (\bar{F}_{55})k_{xz}^s \quad (11)$$

All transformation matrices are presented in Appendix A.

## 2.4 Governing equations

Based on the constitutive equations and Hamilton's principle, equilibrium equations of unified composite sandwich beam rested on elastic foundation and subjected to the in-plane distributed load can be represented by

$$\bar{A}_{11} u_0'' - \bar{B}_{11} w_0''' + \bar{E}_{11} \varphi'' = 0 \quad (12a)$$

$$\begin{aligned} \bar{B}_{11} u_0''' - \bar{D}_{11} w_0'''' + \bar{F}_{11} \varphi''' \\ + N_{amp} [C(x)w_0' - R(x)w_0''] \\ + K_w w_0 - K_p w_0'' = 0 \end{aligned} \quad (12b)$$

$$\bar{F}_{55} \varphi - \bar{E}_{11} u_0'' + \bar{F}_{11} w_0''' - \bar{H}_{11} \varphi'' = 0 \quad (12c)$$

in which, the axial load and its variation can be computed by

$$\begin{aligned} R(x) = \int_{\bar{x}=x}^{\bar{x}=L/2} N_{axial}(\bar{x}) d\bar{x} = N_{amp} \left( \frac{\alpha_2}{3} L^3 + \frac{\alpha_1}{2} L^2 + \right. \\ \left. \frac{\alpha_0}{2} L - \left( \frac{\alpha_2}{3} \left(x + \frac{L}{2}\right)^3 + \frac{\alpha_1}{2} \left(x + \frac{L}{2}\right)^2 + \alpha_0 x \right) \right) \end{aligned} \quad (13a)$$

$$\begin{aligned} \frac{dR(x)}{dx} = -N_{amp} \left( \alpha_2 \left(x + \frac{L}{2}\right)^2 + \alpha_1 \left(x + \frac{L}{2}\right) + \alpha_0 \right) = \\ -N_{amp} C(x) \end{aligned} \quad (13b)$$

The boundary conditions for sandwich composite beam can be evaluated by

$$[\bar{A}_{11} u_0' - \bar{B}_{11} w_0'' + \bar{E}_{11} \varphi'] \delta u_0 = 0 \quad (14a)$$

$$\begin{aligned} [-\bar{B}_{11} u_0'' + \bar{D}_{11} w_0''' - \bar{F}_{11} \varphi'' \\ + N_{amp} R(x)w_0'] \delta w_0 = 0 \end{aligned} \quad (14b)$$

$$[-\bar{E}_{11} u_0' + \bar{F}_{11} w_0'' - \bar{H}_{11} \varphi'] \delta \varphi = 0 \quad (14c)$$

$$[\bar{B}_{11} u_0' - \bar{D}_{11} w_0'' + \bar{F}_{11} \varphi'] \delta w_0' = 0 \quad (14d)$$

where  $K_w$  and  $K_p$  are the spring constants of the Winkler and Pasternak elastic medium, respectively.

## 3. Solution procedure

Due to the simplicity and efficiency of the differential quadrature method (DQM) is used in solving the differential equations used in many engineering applications [buckling,

post-buckling and free vibration of imperfect beam Mohamed *et al.* (2018), buckling and postbuckling of CNTs Eltaher (2019b), stability of periodic and non-periodic imperfect beams Eltaher *et al.* (2019c)], therefore, DQM is proposed as solution technique to solve the current model.

The governing equations of motion of unified composite beam under the axial distributed load Eq. (12) and corresponding boundary conditions Eq. (14) are solved by the differential quadrature method DQM. Let the beam length be discretized using  $N$  nodes. The Chebyshev–Gauss–Lobatto distribution of the discrete nodes on the beam is employed such that

$$x_i = -\frac{L}{2} + \frac{L}{2} \left(1 - \cos\left(\pi \frac{i-1}{N-1}\right)\right), \quad i = 1, 2, \dots, N \quad (15)$$

Using the DQM, different order derivatives of a function at a given node can be approximated using a weighted sum of the function values at all discrete nodes in its domain. The first order derivative of function  $f(x)$  at node  $x_i$  can be approximated using the DQM as follows

$$\left. \frac{df}{dx} \right|_{x=x_i} = \sum_{j=1}^N d_{ij} f_j, \quad i = 1, 2, \dots, N \quad (16)$$

where  $f_j = f(x_j)$  and  $d_{ij}$  denote the corresponding weighting coefficients. The weighting coefficients can be expressed as follows, Shu (2000)

$$d_{ij} = \frac{1}{x_j - x_i} \left( \frac{P_i}{P_j} \right), \quad i \neq j \quad \text{and} \quad (17)$$

$$d_{ii} = -\sum_{j=1, j \neq i}^N d_{ij}$$

in which

$$P_i = \prod_{j=1, j \neq i}^N (x_i - x_j), \quad i, j = 1, 2, \dots, N \quad (18)$$

In matrix form, let the discrete values of  $f_i = f(x_i)$  at different nodes be given as a vector  $f = [f_1, f_2, \dots, f_N]^T$ . Also, let its first derivative vector be  $F$ , then

$$F = \mathcal{D}^{(1)} f \quad (19)$$

where  $\mathcal{D}^{(1)} = [d_{ij}]$  is the weighting  $N \times N$  matrix of the first order derivative. The weighting coefficients matrices for higher-order derivatives can be determined via matrix multiplication. Let the matrices  $\mathcal{D}^{(1)}, \mathcal{D}^{(2)}, \mathcal{D}^{(3)}$  and  $\mathcal{D}^{(4)}$  be respectively the coefficients matrices corresponding to the first, second, third and fourth derivatives. The unknown variables in Eq. (12) are discretized to three unknown vectors  $U = [u_1, u_2, \dots, u_i, \dots, u_N]^T$ ,  $W = [w_1, w_2, \dots, w_i, \dots, w_N]^T$ , and  $\varphi = [\varphi_1, \varphi_2, \dots, \varphi_i, \dots, \varphi_N]^T$  where  $u_i = u_0(x_i)$ ,  $w_i = w_0(x_i)$  and  $\varphi_i = \varphi_0(x_i)$ ,  $i = 1, 2, \dots, N$ . Also, the given axial load functions  $C(x)$  and  $R(x)$  appearing in Eq. 13 are discretized respectively as known vectors  $C = [c_1, c_2, \dots, c_i, \dots, c_N]^T$  and  $R = [r_1, r_2, \dots, r_i, \dots, r_N]^T$ .

Accordingly, terms as  $u_0''', w_0''', \varphi''$  are discretized respectively by the vectors  $\mathcal{D}^{(1)}U, \mathcal{D}^{(3)}W$  and  $\mathcal{D}^{(2)}\varphi$ . However, to discretize the function  $(R(x)w_0'' - C(x)w_0')$  in Eq. (30b), special matrices multiplications operators are

essential. The first is the element by element operator ' $\circ$ ' defined for matrices  $\mathcal{A}, \mathcal{B}, \mathcal{C}$  having the same dimensions such that  $\mathcal{C} = \mathcal{A} \circ \mathcal{B}$  implies that  $C_{ij} = A_{ij} B_{ij}$ . The second is the vector matrix multiplication operator ' $\otimes$ ' defined for a vector  $\mathcal{V}$  and matrix  $\mathcal{A}$  having the same number of rows such that  $\mathcal{C} = \mathcal{V} \otimes \mathcal{A}$  implies that  $C_{ij} = V_i A_{ij}$ . The discrete vector of  $(R(x)w_0'' - C(x)w_0')$  is given by  $V = R \circ (\mathcal{D}^{(2)}W) - C \circ (\mathcal{D}^{(1)}W)$ . Using the operator  $\otimes$ , this vector can be better written as  $V = (R \otimes \mathcal{D}^{(2)})W - (C \otimes \mathcal{D}^{(1)})W$  or as  $V = SW$  where matrix  $S$  is defined by

$$S = (R \otimes \mathcal{D}^{(2)}) - (C \otimes \mathcal{D}^{(1)}) \quad (20)$$

The discrete algebraic system corresponding to Eqs. (12) can now be written as

$$\begin{bmatrix} \bar{A}_{11} \mathcal{D}^{(2)} & -\bar{B}_{11} \mathcal{D}^{(3)} & \bar{E}_{11} \mathcal{D}^{(2)} \\ \bar{B}_{11} \mathcal{D}^{(3)} & -\bar{D}_{11} \mathcal{D}^{(4)} + K_w I - K_p \mathcal{D}^{(2)} & \bar{F}_{11} \mathcal{D}^{(3)} \\ -\bar{E}_{11} \mathcal{D}^{(2)} & \bar{F}_{11} \mathcal{D}^{(3)} & \bar{F}_{55} I - \bar{H}_{11} \mathcal{D}^{(2)} \end{bmatrix} \begin{bmatrix} U \\ W \\ \varphi \end{bmatrix} = \begin{bmatrix} 0 & 0 & 0 \\ 0 & S & 0 \\ 0 & 0 & 0 \end{bmatrix} \begin{bmatrix} U \\ W \\ \varphi \end{bmatrix} \quad (21)$$

where  $I$  is the identity matrix of order  $N$  and  $O$  is the zero matrix of order  $N \times N$ . The boundary conditions Eq. (14) are discretized and properly substituted into Eq. (21). The resulting system is a generalized eigenvalue problem that can easily be solved for the eigenvalues (buckling loads) and eigenvectors (mode-shapes). The amplitude of fundamental buckling load  $N_{amp}$  is the smallest eigenvalue of the system.

## 4. Numerical results

Numerical studies are devoted to different sections. In the first section, the model will be validated and compared with published papers. Effects of sandwich ratio, load type and slenderness ratio on buckling loads of sandwich beams will be presented and discussed in section two. The effect of elastic foundation parameters on the sandwich beam under varying in-plane load will be illustrated in last section. The beam consider through numerical studies, will have the following material properties  $E_3 = E_2$ ;  $G_{12} = G_{13} = 0.5E_2$ ;  $G_{23} = 0.2E_2$ ;  $\nu_{12} = \nu_{13} = \nu_{23} = 0.25$ , and have clamped-clamped boundary conditions.

### 4.1 Validation

To verify the proposed model, authors adopted previous model of Karamanli and Aydogdu (2019), which was solved by Ritz procedure, to be solved by DQM in the current analysis. The dimensionless critical buckling loads of symmetric  $[0^\circ/\theta/0^\circ]$  composite beam is shown in Table 2. Buckling loads are evaluated at the following conditions:

$$\begin{aligned} \text{slenderness ratio } \frac{L}{h} &= 20, & \text{modulus elasticity} \\ & & \text{ratio } \frac{E_1}{E_2} = 25, \end{aligned}$$

different axial load function, and different angle of orientation.

Table 2 Critical Buckling loads of  $[0^\circ/\theta/0^\circ]$  laminated beam with different axial in plane loads

	Angle	$N_{con}$	$N_{LL}$	$N_{LR}$	$N_{PL}$	$N_{PR}$	$N_{PS}$
<b>Present</b>	0°	47.6967	36.7846	64.0139	33.1590	76.8934	45.5210
<b>Karamanli</b>		47.6910	36.7832	63.9673	33.1581	76.5962	45.5185
<b>Present</b>	30°	45.7375	35.3262	61.1048	31.8632	73.0642	43.6035
<b>Karamanli</b>		45.7322	35.3248	61.0559	31.8623	72.7507	43.6015
<b>Present</b>	45°	43.7170	33.8308	58.0637	30.5377	69.0205	41.6204
<b>Karamanli</b>		43.7122	33.8296	58.0117	30.5369	68.6904	41.6192
<b>Present</b>	60°	41.5712	32.2509	54.8007	29.1402	64.6492	39.5109
<b>Karamanli</b>		41.5672	32.2499	54.7439	29.1395	64.3122	39.5108
<b>Present</b>	90°	39.2181	30.5249	51.2045	27.6157	59.8270	37.1984
<b>Karamanli</b>		39.2151	30.5241	51.1407	27.6152	59.5063	37.1994

Table 3 Critical buckling loads of  $[0^\circ 90^\circ 0^\circ]$  sandwich beam at different beam theories and axial in-plane loads, ( $E_1/E_2 = 25$ )

$L/h$	$h_2/h_1$		Load type					$N_{PS}$
			$N_{con}$	$N_{LL}$	$N_{LR}$	$N_{PL}$	$N_{PR}$	
<b>5</b>	1	PSDBT	5.3464	4.3233	6.6687	3.9902	7.7802	5.0010
		ESDBT	5.6118	4.4746	7.1651	4.1047	8.4827	5.2861
		TSDBT	5.4825	4.4076	6.9093	4.0378	8.1168	5.1298
		HSDBT	5.3434	4.3211	6.6490	3.9965	7.9008	4.9366
	3	PSDBT	3.8618	3.1692	4.7126	2.9452	5.4289	3.6021
		ESDBT	4.0204	3.2600	4.9918	3.0145	5.8045	3.7562
		TSDBT	3.9335	3.2076	4.8566	2.9711	5.6020	3.6687
		HSDBT	3.8594	3.1664	4.7090	2.9434	5.2979	3.6188
	10	PSDBT	3.1662	2.6795	3.6825	2.5206	4.0952	2.9447
		ESDBT	3.3809	2.8317	3.9821	2.6527	4.4771	3.1466
		TSDBT	3.2663	2.7490	3.8249	2.5808	4.2744	3.0414
		HSDBT	3.1508	2.6796	3.6730	2.5263	4.0811	2.9454
<b>20</b>	1	PSDBT	38.7111	30.2847	49.9802	27.4462	57.8950	36.7508
		ESDBT	38.0068	29.7531	49.0885	26.9646	57.0480	36.0659
		TSDBT	38.3397	30.0030	49.4973	27.1884	57.3962	36.3864
		HSDBT	38.7402	30.3057	50.0327	27.4636	57.6423	36.7793
	3	PSDBT	30.7611	24.1366	39.3204	21.8964	44.9843	29.1493
		ESDBT	30.5331	23.9709	39.0760	21.7445	44.8717	28.9467
		TSDBT	30.6087	24.0279	39.1323	21.7939	44.8556	29.0139
		HSDBT	30.7762	24.1517	39.3390	21.9043	45.0134	29.1685
	10	PSDBT	21.8415	16.8626	29.2734	15.2039	35.0237	20.8783
		ESDBT	22.1580	17.0906	29.7944	15.4024	35.7787	21.1987
		TSDBT	21.9859	16.9657	29.5091	15.2935	35.3653	21.0225
		HSDBT	21.8293	16.8559	29.2559	15.1957	34.9948	20.8660

As shown from Table 2, by increasing the orientation angle, the critical buckling loads will be decreased. The maximum buckling load is observed in parabolic variation of load from the right  $N_{PR}$ , however, the minimum critical load is predicted in case of parabolic variation from left  $N_{PL}$ . From this table, the current results are identical with previous work of Karamanli and Aydogdu (2019) within max difference of 0.5%.

## 4.2 Sandwich beam without elastic foundation

### 4.2.1 Effect of shear functions

Effect of proposed shear functions used in beam theories on the critical buckling loads of sandwich orthotropic composite beam  $[0^\circ 90^\circ 0^\circ]$  with varying load, varying slenderness ratio, and varying the thickness of the core layer are presented in Table 3. As noticed, the higher buckling load is observed in case of exponential shear distribution (ESDBT) and the lowest buckling load is detected for

Table 4 The First three buckling loads of sandwich beam ( $E_1/E_2 = 25, \theta = [0^\circ 90^\circ 0^\circ]$ ) with different slenderness and sandwich ratios

Slenderness Ratio	Sandwich Ratio	mode	Axial load type					
			$N_{con}$	$N_{LL}$	$N_{LR}$	$N_{PL}$	$N_{PR}$	$N_{PS}$
$L/h = 5$	$h_2/h_1 = 3$	1	4.0204	3.2600	4.9918	3.0145	5.8045	3.7562
		2	5.029	3.839	6.820	3.479	8.571	4.642
		3	6.255	5.148	9.704	4.450	13.108	6.593
	$h_2/h_1 = 8$	1	3.420	2.859	4.051	2.666	4.553	3.182
		2	4.001	3.178	5.091	2.929	6.113	3.661
		3	4.998	3.886	6.701	3.410	8.080	4.644
$L/h = 20$	$h_2/h_1 = 3$	1	30.5331	23.9709	39.0760	21.7445	44.8717	28.9467
		2	38.136	30.591	46.874	28.054	54.068	35.436
		3	47.815	39.567	58.519	36.801	68.124	44.798
	$h_2/h_1 = 8$	1	24.009	18.582	31.931	16.769	37.899	22.913
		2	27.702	21.432	37.236	19.358	44.953	26.385
		3	32.801	25.831	40.883	23.492	46.858	30.631
$L/h = 50$	$h_2/h_1 = 3$	1	51.823	39.341	73.246	35.218	92.720	50.209
		2	92.861	69.069	134.202	61.521	172.540	88.611
		3	155.913	119.743	212.074	107.403	252.285	151.533
	$h_2/h_1 = 8$	1	34.887	26.411	49.701	23.627	63.394	33.853
		2	65.850	48.559	97.848	43.108	129.899	63.212
		3	117.764	89.068	168.555	79.425	210.737	115.863

hyperbolic shear distribution (HSDBT). It is also noted that, the buckling loads for parabolic shear distribution (PSDBT) and hyperbolic shear are much closer to each other. The buckling load for trigonometry shears function (TSDBT) lies between PSDBT and ESDBT.

From Table 3, it is noticed that, the highest buckling load is observed in case of  $N_{PR}$  and the minimum critical load is found at  $N_{PL}$ , at the same other conditions. So that, the parabolic in-plane load function is the most significant function on the buckling loads rather than the linear and constant functions.

#### 4.2.2 Effect of sandwich core thickness

It is observed from Table 3, in case of  $L/h=5$ , PSDBT and  $N_{con}$  by increasing  $h_2/h_1$  from 1 to 10, the buckling load will be decreased 5.3464 to 3.1662, which means a reduction of buckling loads by 40%. So that, as the thickness of core increased the buckling load will be decreased. This reduction due to the increasing of the thickness of the  $90^\circ$  layer, which has a less stiffness rather than surface layers those have  $0^\circ$ .

#### 4.2.3 Higher buckling loads

Influences of sandwich thickness, slenderness ratio, load functions on the 1<sup>st</sup> three buckling critical buckling loads of  $[0^\circ 90^\circ 0^\circ]$  sandwich beam structure are presented in Table 4. As predicted from the table, the critical buckling loads are more pronounced by the slenderness ratio rather than sandwich thickness and load function. It is noticed, by

increasing the slenderness ratio from 5 to 20; the 1<sup>st</sup> buckling load will be increased from 4.02 to 30.53, the 2<sup>nd</sup> buckling load increased from 5.029 to 38.136, and the 3<sup>rd</sup> buckling load increased from 6.255 to 47.815, at  $N_{con}$  and  $h_2/h_1 = 3$ . It is noted at  $L/h = 5$  and load function of  $N_{con}$ , as the sandwich thickness increases from 3 to 8, the 1<sup>st</sup> buckling load will be decreased from 4.02 to 3.42, the 2<sup>nd</sup> buckling load will be reduced from 5.029 to 4.0 and the 3<sup>rd</sup> buckling load will be decreased from 6.255 to 4.998.

Thus, it can be concluded that, the critical buckling loads increased by increasing the slenderness ratio and decreasing the sandwich ratio of sandwich beam structures.

The variation of the 1<sup>st</sup> buckling mode with respect to the in-plane axial load function is presented in Fig. 2. As presented, the mode-shapes are non-symmetric due to the type in-plane load function. The parabolic function changing from the right  $N_{PR}$  is the most significant mode distorted mode from symmetric position, and the parabolic function from the left  $N_{PL}$  is the closet mode to symmetry position.

The effect of the in-plane load function on the first three mode shapes of sandwich clamped beam is illustrated in Fig. 3. As shown, normalized deflection of the 1<sup>st</sup>, 2<sup>nd</sup> and third mode shapes for each load function are plotted in the same figure. It is noted that, all modes for the six in-plane load function are nonsymmetric from the normal modes, and all of them are shifted to the left. The  $N_{PR}$  load function is the most effective load function on the three mode shapes.

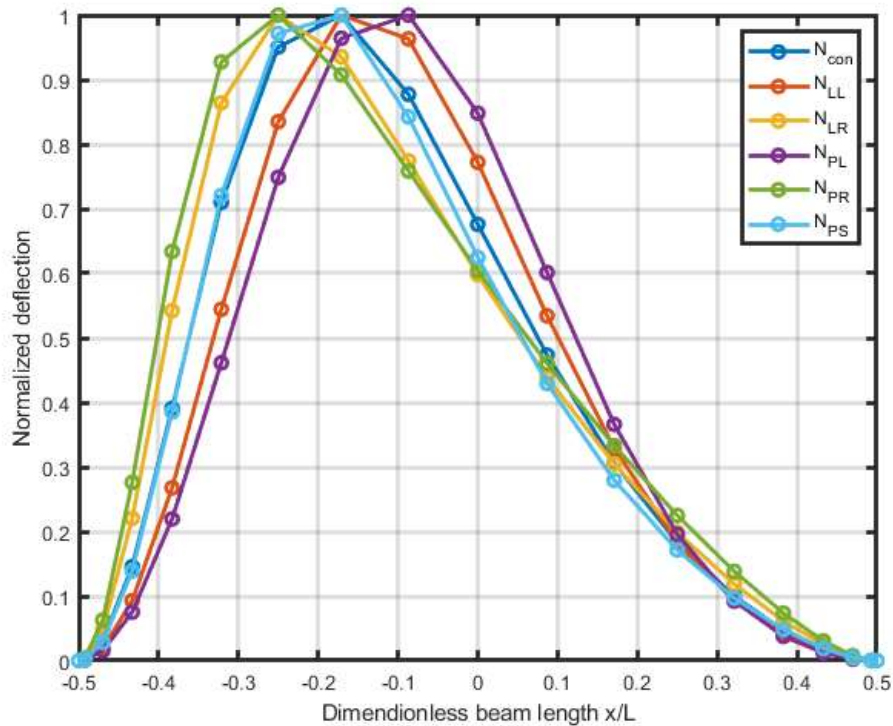


Fig. 2 Variation of 1<sup>st</sup> mode shape of clamped-clamped  $[0^\circ 90^\circ 0^\circ]$  sandwich beam vs different load functions at  $E_1/E_2 = 25$ ;  $h_2/h_1 = 3$ ;  $L/h = 20$

#### 4.3 Sandwich beam with elastic foundation

This section is devoted to illustrating the influence of elastic foundation constants on the critical buckling loads of clamped sandwich beam under different in-plane load function, sandwich ratio. These influences are presented in Tables 5 and 6 at slenderness ratios  $L/h$  of 5 and 20, respectively. The qualitative presentations of these tables are presented in Figs. 4-7.

As shown in Fig. 4, the critical buckling load is decreased by increasing the sandwich ratio, due to increasing the thickness of the core material that has lower stiffness relative to the face layers that have the higher stiffnesses. The highest buckling load is observed in case of  $N_{PR}$  loading function. It is observed by increasing the Pasternak foundation constant  $\bar{K}_p$ , the critical buckling load is decreased, at the same other parameters (load type, sandwich ratio, slenderness ratio and Winkler parameter). From Fig. 5, which represent the effect of Winkler parameter on the critical buckling loads, it can be concluded that, the Winkler parameter tends to decrease the critical buckling load at the same other parameters. The same effect observed in case of Pasternak parameter on the buckling load is noticed in case of Winkler parameter. So, the Pasternak and Winkler parameters have the same effect on the critical buckling loads of sandwich beam.

#### 5. Conclusions

The buckling stability and associated mode-shapes of the sandwich laminated beam rested on the Winkler and Pasternak elastic foundation and subjected to in-plane axial load with different distribution function is the main investigation of this article. Unified shear deformation theories are exploited to describe the displacement field of the beam and satisfied the zero shear effect at the top and bottom surface of the sandwich beam.

Numerical differential quadrature method (DQM) with the Chebyshev–Gauss–Lobatto distribution is used to solve equilibrium equations, then derive the critical buckling loads and their mode-shapes. The interesting points of this study can be summarized as follows:-

- *Shear Function Distribution*:- the higher buckling load is observed in case of exponential shear distribution and the lowest buckling load is detected for hyperbolic shear distribution. It is also noted that, the buckling loads for parabolic shear distribution (PSDBT) and hyperbolic shear are very closed to each other.

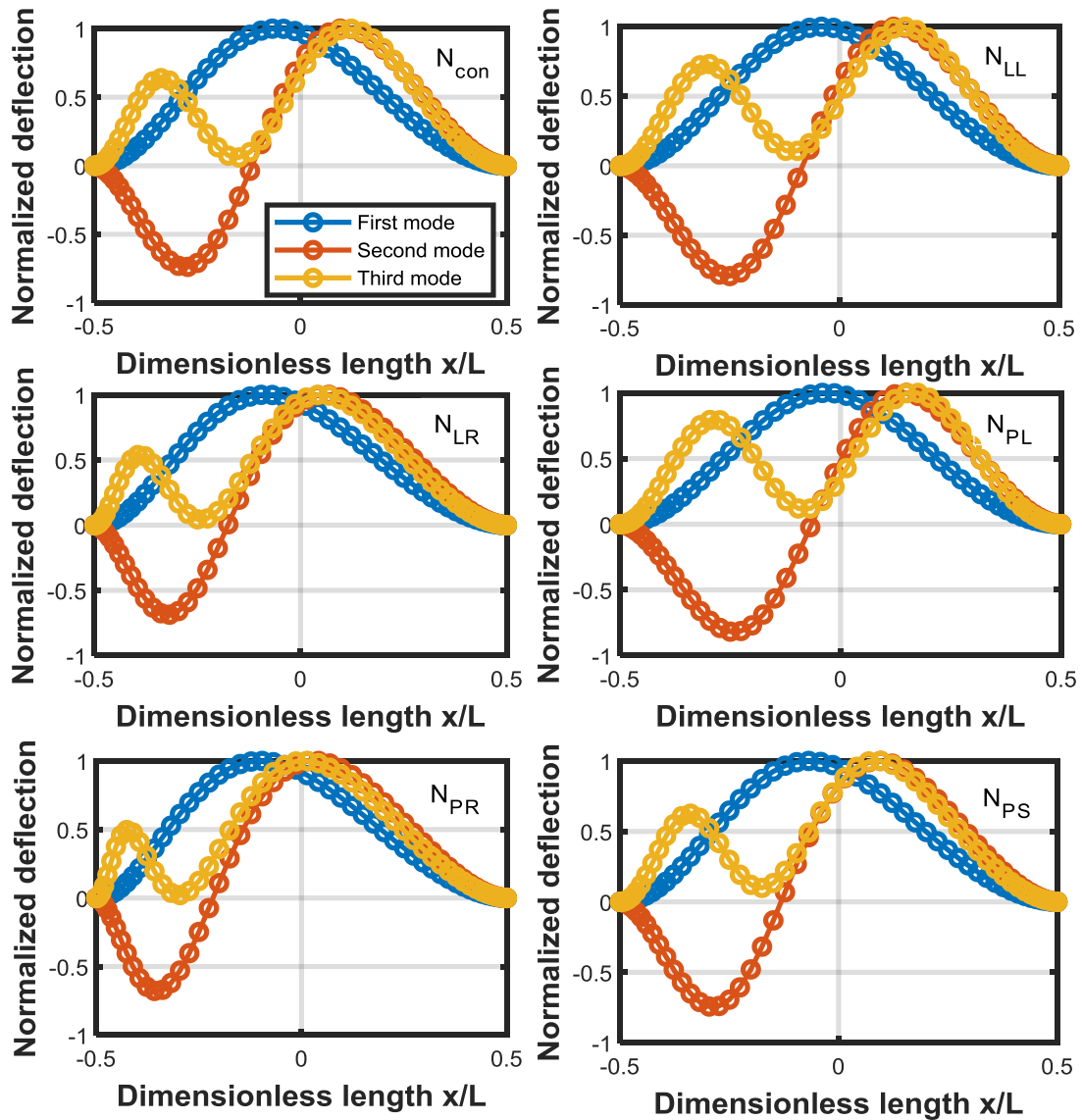


Fig. 3 The 1<sup>st</sup> three mode shapes of  $[0^\circ 90^\circ 0^\circ]$  sandwich beam for different load functions at  $E_1/E_2 = 25$ ;  $h_2/h_1 = 3$ ;  $L/h = 50$

- *In-plane Load Function Distribution*:- the highest buckling load is observed in case of  $N_{PR}$  and the minimum critical load is found at  $N_{PL}$ , at the same other conditions. So that, the parabolic in-plane load function is the most significant function on the buckling loads rather than the linear and constant functions.
- *Beam Geometry*:- the critical buckling loads are more pronounced by the slenderness ratio rather than sandwich thickness and load function.
- *Mode-Shape*:- the parabolic function changing from the right  $N_{PR}$  is the most significant mode distorted mode from symmetric position, and the parabolic function from the left  $N_{PL}$  is the closet mode to symmetry position.

- *Elastic Foundation*:- the Pasternak and Winkler parameters have the same effect on the critical buckling loads of sandwich beam, those tend to decrease the critical buckling loads by increasing their parameters.

#### Acknowledgments

This work was funded by the Deanship of Scientific Research (DSR), King Abdulaziz University, Jeddah, under grant No. (D-298-135-1440). The authors, therefore, acknowledge with thanks DSR technical and financial support.

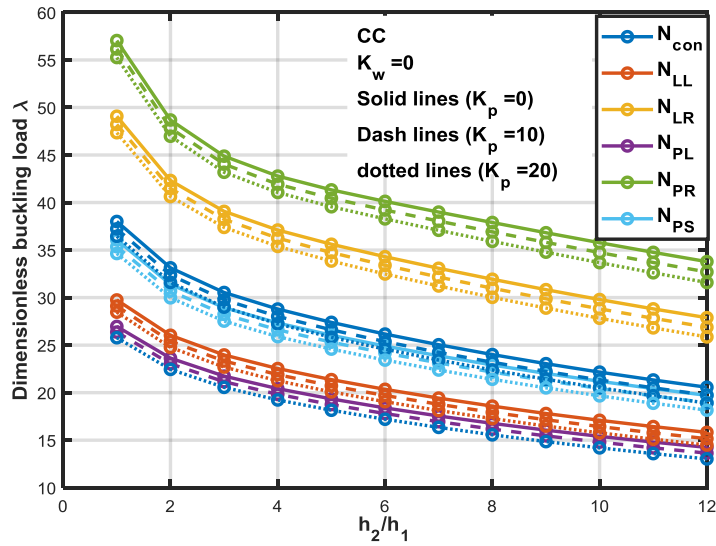


Fig. 4 Effect of Pasternak foundation constant  $\bar{K}_p$  and sandwich ratio on critical buckling load of clamped-clamped sandwich beam  $\theta = [0^\circ/90^\circ/0^\circ]$ , for different types of axial loads. ( $E_1/E_2 = 25, L/h = 20$ )

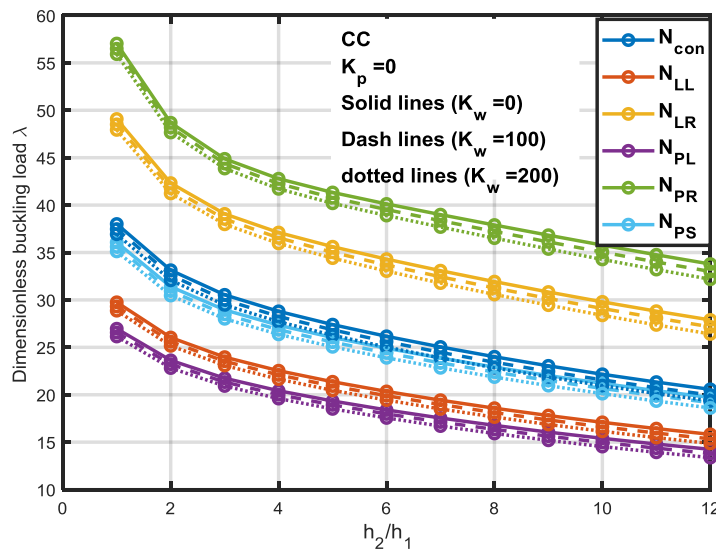


Fig. 5 Effect of Pasternak foundation constant  $\bar{K}_w$  and sandwich ratio on critical buckling load of clamped-clamped sandwich beam  $\theta = [0^\circ/90^\circ/0^\circ]$ , for different types of axial loads. ( $E_1/E_2 = 25, L/h = 20$ )

Table 5 Effect of foundation parameters on the dimensionless critical buckling loads of symmetric  $[0^\circ/90^\circ/0^\circ]$  sandwich beam subjected to different axial in plane loads and different sandwich ratios,  $[(E_1/E_2 = 25) , L/h=5]$ 

$h_2/h_1$	$K_p$	$K_w$	Load type						
			$N_{con}$	$N_{LL}$	$N_{LR}$	$N_{PL}$	$N_{PR}$	$N_{PS}$	
<b>1</b>	0	0	5.6126	4.4742	7.1649	4.1042	8.4829	5.2866	
		20	5.2370	4.1586	6.7520	3.8018	8.0186	4.9462	
		50	4.5917	3.6207	6.0098	3.2954	7.2018	4.3732	
	5	0	4.1280	3.2447	5.4064	2.9555	6.4209	3.9020	
		20	3.7038	2.9189	4.9188	2.6288	5.9496	3.5306	
		50	2.9661	2.3028	4.0281	2.0819	4.9627	2.8617	
	8	0	3.1971	2.4856	4.2768	2.2512	5.1684	3.0392	
		20	2.7334	2.1336	3.7350	1.9068	4.5920	2.6296	
		50	1.9350	1.4820	2.7051	1.3319	3.3260	1.8844	
	<b>3</b>	0	0	4.0202	3.2604	4.9920	3.0148	5.8050	3.7561
			20	3.6834	2.9695	4.6294	2.7327	5.4069	3.4673
			50	3.0466	2.4259	3.9207	2.2154	4.6369	2.9044
5		0	2.6035	2.0654	3.3434	1.8905	3.9729	2.4525	
		20	2.1859	1.7219	2.8778	1.5665	3.4525	2.0847	
		50	1.4017	1.0872	1.9149	0.9810	2.3606	1.3620	
8		0	1.6916	1.3179	2.2544	1.1957	2.7496	1.6071	
		20	1.2034	0.9286	1.6614	0.8382	2.0689	1.1665	
		50	0.2969	0.2264	0.4310	0.2009	0.5815	0.2953	
<b>10</b>		0	0	3.3809	2.8316	3.9821	2.6528	4.4771	3.1467
			20	3.1122	2.5785	3.7212	2.3974	4.1972	2.9194
			50	2.5137	2.0406	3.1194	1.8756	3.5768	2.3980
	5	0	2.0699	1.6871	2.5346	1.5596	2.9095	1.9359	
		20	1.7014	1.3639	2.1436	1.2483	2.5082	1.6161	
		50	0.8874	0.6954	1.1960	0.6288	1.4501	0.8677	
	8	0	1.2191	0.9648	1.5673	0.8800	1.8564	1.1525	
		20	0.7399	0.5738	1.0062	0.5174	1.2315	0.7177	
		50	0.2615	0.1991	0.3862	0.1772	0.5091	0.2639	

Table 6 Effect of foundation parameters on the dimensionless critical buckling loads of symmetric  $[0^\circ/90^\circ/0^\circ]$ s andwich beam subjected to different axial in plane loads and different sandwich ratios,  $[(E_1/E_2 = 25)$  ,  $L/h=20$  ]

$h_2/h_1$	$K_p$	$K_w$	Load type					
			$N_{con}$	$N_{LL}$	$N_{LR}$	$N_{PL}$	$N_{PR}$	$N_{PS}$
<b>1</b>	0	0	38.0053	29.7512	49.0810	26.9639	57.0413	36.0695
		100	37.4698	29.3111	48.5141	26.5561	56.4916	35.5988
		200	36.9231	28.8648	47.9310	26.1421	55.9211	35.1167
	10	0	37.2314	29.1113	48.2159	26.3719	56.1540	35.3559
		100	36.6914	28.6691	47.6398	25.9626	55.5928	34.8796
		200	36.1404	28.2202	47.0494	25.5469	55.0109	34.3937
	20	0	36.4538	28.4700	47.3461	25.7792	55.2572	34.6382
		100	35.9088	28.0256	46.7607	25.3677	54.6845	34.1569
		200	35.3540	27.5739	46.1587	24.9504	54.0903	33.6666
<b>3</b>	0	0	30.5378	23.9676	39.0736	21.7422	44.8773	28.9468
		100	30.0093	23.5318	38.5342	21.3366	44.3803	28.4850
		200	29.4675	23.0865	37.9677	20.9233	43.8563	28.0093
	10	0	29.7706	23.3306	38.2344	21.1516	44.0368	28.2396
		100	29.2359	22.8917	37.6824	20.7442	43.5235	27.7716
		200	28.6889	22.4437	37.1050	20.3288	42.9849	27.2900
	20	0	28.9989	22.6917	37.3867	20.5598	43.1848	27.5282
		100	28.4586	22.2496	36.8179	20.1499	42.6567	27.0541
		200	27.9057	21.7980	36.2323	19.7324	42.1004	26.5662
<b>10</b>	0	0	22.1602	17.0911	29.7951	15.4019	35.7775	21.1971
		100	21.5681	16.6219	29.0962	14.9723	35.0426	20.6640
		200	20.9634	16.1431	28.3739	14.5355	34.2699	20.1177
	10	0	21.3404	16.4316	28.8175	14.7998	34.7447	20.4364
		100	20.7435	15.9600	28.1061	14.3689	33.9843	19.8969
		200	20.1298	15.4774	27.3676	13.9287	33.1917	19.3414
	20	0	20.5145	15.7714	27.8280	14.1931	33.6765	19.6659
		100	19.9121	15.2951	27.1004	13.7589	32.8945	19.1186
		200	19.2935	14.8103	26.3489	13.3176	32.0754	18.5569

## References

- Abdalrahmaan, A.A., Eltahaer, M.A., Kabeel, A.M., Abdraboh, A.M. and Hendi, A.A. (2019), "Free and forced analysis of perforated beams", *Steel Compos. Struct.*, **31**(5), 489-502. <https://doi.org/10.12989/scs.2019.31.5.489>.
- Akbas, S.D. (2018a), "Geometrically nonlinear analysis of a laminated composite beam", *Struct. Eng. Mech.*, **66**(1), 27-36. <https://doi.org/10.12989/sem.2018.66.1.27>.
- Akbas, S.D. (2018b), "Post-buckling responses of a laminated composite beam", *Steel Compos. Struct.*, **26**(6), 733-743. <https://doi.org/10.12989/scs.2018.26.6.733>.
- Akbas, S.D. (2018c), "Nonlinear thermal displacements of laminated composite beams", *Coupled Syst. Mech.*, **7**(6), 691-705. <https://doi.org/10.12989/csm.2018.7.6.691>.
- Akbas, Ş.D. (2019a), "Hygrothermal post-buckling analysis of laminated composite beams", *Int. J. Appl. Mech.*, **11**(1), 1950009. <https://doi.org/10.1142/S1758825119500091>.
- Akbas, Ş.D. (2019b), "Hygro-thermal post-buckling analysis of a functionally graded beam", *Coupled Syst. Mech.*, **8**(5), 459-471. <https://doi.org/10.12989/csm.2019.8.5.459>.
- Almitani, K.H., Abdalrahmaan, A.A. and Eltahaer, M.A. (2019), "On forced and free vibrations of cutout squared beams", *Steel Compos. Struct.*, **32**(5), 643-655. <https://doi.org/10.12989/scs.2019.32.5.643>.
- Assie, A.E., Eltahaer, M.A. and Mahmoud, F.F. (2011), "Behavior of a viscoelastic composite plates under transient load", *J. Mech. Sci. Technol.*, **25**(5), 1129. <https://doi.org/10.1007/s12206-011-0302-6>.
- Bessaim, A., Ahmed Houari, M.S., Abdelmoumen Anis, B., Kaci, A., Tounsi, A., Bedia, A. and Abbes, E. (2018), "Buckling analysis of embedded nanosize FG beams based on a refined hyperbolic shear deformation theory", *J. Appl. Comput. Mech.*, **4**(3), 140-146.
- Dehrouyeh-Semnani, A.M. (2018), "On the thermally induced non-linear response of functionally graded beams", *Int. J. Eng. Sci.*, **125**, 53-74. <https://doi.org/10.1016/j.ijengsci.2017.12.001>.
- Eltahaer, M.A., Emam, S.A. and Mahmoud, F.F. (2012), "Free vibration analysis of functionally graded size-dependent nanobeams", *Appl. Math. Comput.*, **218**(14), 7406-7420. <https://doi.org/10.1016/j.amc.2011.12.090>.
- Eltahaer, M.A., Emam, S.A. and Mahmoud, F.F. (2013a), "Static and stability analysis of nonlocal functionally graded nanobeams", *Compos. Struct.*, **96**, 82-88. <https://doi.org/10.1016/j.compstruct.2012.09.030>.
- Eltahaer, M.A., Alshorbagy, A.E. and Mahmoud, F.F. (2013b), "Determination of neutral axis position and its effect on natural frequencies of functionally graded macro/nanobeams", *Compos. Struct.*, **99**, 193-201.
- Eltahaer, M.A., Khairy, A., Sadoun, A.M. and Omar, F.A. (2014a), "Static and buckling analysis of functionally graded Timoshenko nanobeams", *Appl. Math. Comput.*, **229**, 283-295. <https://doi.org/10.1016/j.amc.2013.12.072>.
- Eltahaer, M.A., Abdelrahman, A.A., Al-Nabawy, A., Khater, M. and Mansour, A. (2014b), "Vibration of nonlinear graduation of nano-Timoshenko beam considering the neutral axis position", *Appl. Math. Comput.*, **235**, 512-529. <https://doi.org/10.1016/j.amc.2014.03.028>.
- Eltahaer, M.A., Mohamed, N., Mohamed, S. and Seddek, L.F. (2019a), "Postbuckling of curved carbon nanotubes using energy equivalent model", *J. Nano Res.*, **57**, 136-157. <https://doi.org/10.4028/www.scientific.net/JNanoR.57.136>.
- Eltahaer, M.A., Mohamed, N., Mohamed, S.A. and Seddek, L.F. (2019b), "Periodic and nonperiodic modes on postbuckling and nonlinear vibration of beams attached with nonlinear foundations", *Appl. Math. Model.*, **75**, 414-445.
- Eltahaer, M.A., Mohamed, S.A. and Melaibari, A. (2020), "Static stability of a unified composite beams under varying axial loads", *Thin Wall. Struct.*, **147**, 106488. <https://doi.org/10.1016/j.tws.2019.106488>.
- Emam, S. and Eltahaer, M.A. (2016), "Buckling and postbuckling of composite beams in hygrothermal environments", *Compos. Struct.*, **152**, 665-675. <https://doi.org/10.1016/j.compstruct.2016.05.029>.
- Emam, S., Eltahaer, M., Khater, M. and Abdalla, W. (2018), "Postbuckling and free vibration of multilayer imperfect nanobeams under a pre-stress load", *Appl. Sci.*, **8**(11), 2238. <https://doi.org/10.3390/app8112238>.
- Farajpour, A., Shahidi, A.R., Mohammadi, M. and Mahzoon, M. (2012), "Buckling of orthotropic micro/nanoscale plates under linearly varying in-plane load via nonlocal continuum mechanics", *Compos. Struct.*, **94**(5), 1605-1615. <https://doi.org/10.1016/j.compstruct.2011.12.032> Get rights and content.
- Hamed, M., Sadoun A.M. and Eltahaer, M.A., (2019), "Effects of porosity models on static behavior of size dependent functionally graded beam", *Struct. Eng. Mech.*, **71**(1), 89-98. <https://doi.org/10.12989/sem.2019.71.1.089>.
- Hu, H., Badir, A. and Abatan, A. (2003), "Buckling behavior of a graphite/epoxy composite plate under parabolic variation of axial loads", *Int. J. Mech. Sci.*, **45**(6-7), 1135-1147. <https://doi.org/10.1016/j.ijmecsci.2003.08.003>.
- Jun, L., Xiang, H. and Xiaobin, L. (2016), "Free vibration analyses of axially loaded laminated composite beams using a unified higher-order shear deformation theory and dynamic stiffness method", *Compos. Struct.*, **158**, 308-322. <https://doi.org/10.1016/j.compstruct.2016.09.012>.
- Jun, L., Li, J. and Xiaobin, L. (2017), "A spectral element model for thermal effect on vibration and buckling of laminated beams based on trigonometric shear deformation theory", *Int. J. Mech. Sci.*, **133**, 100-111. <https://doi.org/10.1016/j.ijmecsci.2017.07.059>.
- Karamanli, A. and Aydogdu, M. (2019), "Buckling of laminated composite and sandwich beams due to axially varying in-plane loads", *Compos. Struct.*, **210**, 391-408. <https://doi.org/10.1016/j.compstruct.2018.11.067>.
- Khater, M.E., Eltahaer, M.A., Abdel-Rahman, E. and Yavuz, M. (2014), "Surface and thermal load effects on the buckling of curved nanowires", *Eng. Sci. Technol. Int. J.*, **17**(4), 279-283. <https://doi.org/10.1016/j.jestch.2014.07.003>.
- Kim, N.I., Shin, D.K. and Park, Y.S. (2010), "Coupled stability analysis of thin-walled composite beams with closed cross-section", *Thin Wall. Struct.*, **48**(8), 581-596. <https://doi.org/10.1016/j.tws.2010.03.006>.
- Li, C., Shen, H.S. and Wang, H. (2019), "Thermal post-buckling of sandwich beams with functionally graded negative Poisson's ratio honeycomb core", *Int. J. Mech. Sci.*, **152**, 289-297. <https://doi.org/10.1016/j.ijmecsci.2019.01.002>.
- Mijušković, O., Čorić, B. and Šćepanović, B. (2014), "Exact stress functions implementation in stability analysis of plates with different boundary conditions under uniaxial and biaxial compression", *Thin Wall. Struct.*, **80**, 192-206. <https://doi.org/10.1016/j.tws.2014.03.006>.
- Mohamed, N., Eltahaer, M.A., Mohamed, S.A. and Seddek, L.F. (2018), "Numerical analysis of nonlinear free and forced vibrations of buckled curved beams resting on nonlinear elastic foundations", *Int. J. Non-Linear Mech.*, **101**, 157-173. <https://doi.org/10.1016/j.ijnonlinmec.2018.02.014> Get rights and content.
- Mohamed, N., Eltahaer, M.A., Mohamed, S.A. and Seddek, L.F. (2019), "Energy equivalent model in analysis of postbuckling of imperfect carbon nanotubes resting on nonlinear elastic foundation", *Struct. Eng. Mech.*, **70**(6), 737-750. <https://doi.org/10.12989/sem.2019.70.6.737>.

- Panda, S.K. and Ramachandra, L.S. (2010), "Buckling of rectangular plates with various boundary conditions loaded by non-uniform in-plane loads", *Int. J. Mech. Sci.*, **52**(6), 819-828. <https://doi.org/10.1016/j.ijmecsci.2010.01.009>.
- Reddy, J.N. (2003), *Mechanics of laminated composite plates and shells: theory and analysis*. CRC press.
- Sedighi, H.M., Shirazi, K.H. and Zare, J. (2012a), "An analytic solution of transversal oscillation of quintic non-linear beam with homotopy analysis method", *Int. J. Non-Linear Mech.*, **47**(7), 777-784. <https://doi.org/10.1016/j.ijnonlinmec.2012.04.008>.
- Sedighi, H.M., Shirazi, K.H., Noghrehabadi, A.R. and Yildirim, A. (2012b), "Asymptotic investigation of buckled beam nonlinear vibration. Iranian Journal of Science and Technology", *T. Mech. Eng.*, **36**(M2), 107-116.
- Sedighi, H.M. and Daneshmand, F. (2014), "Nonlinear transversely vibrating beams by the homotopy perturbation method with an auxiliary term", *J. Appl. Comput. Mech.*, **1**(1), 1-9.
- She, G.L., Yuan, F.G. and Ren, Y.R. (2017), "Thermal buckling and post-buckling analysis of functionally graded beams based on a general higher-order shear deformation theory", *Appl. Math. Model.*, **47**, 340-357. <https://doi.org/10.1016/j.apm.2017.03.014>.
- She, G.L., Ren, Y.R., Xiao, W.S. and Liu, H. (2018a), "Study on thermal buckling and post-buckling behaviors of FGM tubes resting on elastic foundations", *Struct. Eng. Mech.*, **66**(6), 729-736. <https://doi.org/10.12989/sem.2018.66.6.729>.
- She, G.L., Yan, K.M., Zhang, Y.L., Liu, H.B. and Ren, Y.R. (2018b), "Wave propagation of functionally graded porous nanobeams based on non-local strain gradient theory", *Eur. Phys. J. Plus*, **133**(9), 368.
- She, G.L., Jiang, X.Y. and Karami, B. (2019a), "On thermal snap-buckling of FG curved nanobeams", *Mater. Res. Express*, **6**(11), 115008.
- She, G.L., Ren, Y.R. and Yan, K.M. (2019b), "On snap-buckling of porous FG curved nanobeams", *Acta Astronautica*, **161**, 475-484. <https://doi.org/10.1016/j.actaastro.2019.04.010>.
- Shimpi, R.P., Guruprasad, P.J. and Pakhare, K.S. (2019), "Simple two variable refined theory for shear deformable isotropic rectangular beams", *J. Appl. Comput. Mech.*, 10.22055/JACM.2019.29555.1615.
- Shu, C. (2012), "Differential quadrature and its application in engineering", *Springer Science & Business Media*.
- Şimşek, M. and Reddy, J.N. (2013), "A unified higher order beam theory for buckling of a functionally graded microbeam embedded in elastic medium using modified couple stress theory", *Compos. Struct.*, **101**, 47-58. <https://doi.org/10.1016/j.compstruct.2013.01.017>.
- Soldatos, K.P. and Timarci, T. (1993), "A unified formulation of laminated composite, shear deformable, five-degrees-of-freedom cylindrical shell theories", *Compos. Struct.*, **25**(1-4), 165-171. [https://doi.org/10.1016/0263-8223\(93\)90162-J](https://doi.org/10.1016/0263-8223(93)90162-J).

## Appendix A

The laminated in-plane rigidities ( $A, B, D, E, F, H$ ) and shear rigidity  $F^s$  matrices appearing in Eqs. (12) and (13) are evaluated by the following

$$(A_{ij}, B_{ij}, D_{ij}) = \int_{-h/2}^h \bar{Q}_{ij} [1, z, z^2] dz \quad (A1)$$

$(i, j = 1, 2, 6)$

$$(E_{ij}, F_{ij}, H_{ij}) = \int_{-h/2}^h \bar{Q}_{ij} f(z) [1, z, f(z)] dz \quad (A2)$$

$(i, j = 1, 2, 6)$

$$(F_{44}^s, F_{45}^s, F_{55}^s) = \int_{-h/2}^h g(z) * g(z) [\bar{Q}_{44}, \bar{Q}_{45}, \bar{Q}_{55}] dz \quad (A3)$$

Since the only nonzero force and moment resultant are  $N_x, M_x, P_x$  and  $R_{xz}$ . So, condensed in-plane force, the bending moment, and refined bending moment can be described as functions of strain components and in-plane transformed rigidities as follows

$$\begin{Bmatrix} N_x \\ M_x \\ P_x \end{Bmatrix} = \begin{bmatrix} \bar{A}_{11} & \bar{B}_{11} & \bar{E}_{11} \\ \bar{B}_{11} & \bar{D}_{11} & \bar{F}_{11} \\ \bar{E}_{11} & \bar{F}_{11} & \bar{H}_{11} \end{bmatrix} \begin{Bmatrix} \varepsilon_x^0 \\ k_x^0 \\ k_x^2 \end{Bmatrix} \quad (A4)$$

in which

$$\begin{bmatrix} \bar{A}_{11} & \bar{B}_{11} & \bar{E}_{11} \\ \bar{B}_{11} & \bar{D}_{11} & \bar{F}_{11} \\ \bar{E}_{11} & \bar{F}_{11} & \bar{H}_{11} \end{bmatrix} = \begin{bmatrix} A_{11} & B_{11} & E_{11} \\ B_{11} & D_{11} & F_{11} \\ E_{11} & F_{11} & H_{11} \end{bmatrix} - \begin{bmatrix} A & B & E \\ B & D & F \\ E & F & H \end{bmatrix} \quad (A5)$$

and

$$\begin{bmatrix} A & B & E \\ B & D & F \\ E & F & H \end{bmatrix} = \begin{bmatrix} A_{12} & A_{16} & B_{12} & B_{16} & E_{12} & E_{16} \\ B_{12} & B_{16} & D_{12} & D_{16} & F_{12} & F_{16} \\ E_{12} & E_{16} & F_{12} & F_{16} & H_{12} & H_{16} \end{bmatrix} \begin{bmatrix} A_{22} & A_{26} & B_{22} & B_{26} & E_{22} & E_{26} \\ A_{26} & A_{66} & B_{26} & B_{66} & E_{26} & E_{66} \\ B_{22} & B_{26} & D_{22} & D_{26} & F_{22} & F_{26} \\ B_{26} & B_{66} & D_{26} & D_{66} & F_{26} & F_{66} \\ E_{22} & E_{26} & F_{22} & F_{26} & H_{22} & H_{26} \\ E_{26} & E_{66} & F_{26} & F_{66} & H_{26} & H_{66} \end{bmatrix}^{-1} \begin{bmatrix} A_{12} & B_{12} & E_{12} \\ A_{16} & B_{16} & E_{16} \\ B_{12} & D_{12} & F_{12} \\ B_{16} & D_{16} & F_{16} \\ E_{12} & F_{12} & H_{12} \\ E_{16} & F_{16} & H_{16} \end{bmatrix} \quad (A6)$$

and the shear force resultant

$$\{R\} = [F^s] \{k^s\} \quad (A7)$$